Available online at www.sciencedirect.com
ScienceDirect
Biochimica et Biophysica Acta 1767 (2007) 170–177
Biochimica et Biophysica Acta BBA
www.elsevier.com/locate/bbabio

Cell surface oxygen consumption: A major contributor to cellular oxygen consumption in glycolytic cancer cell lines

Patries M. Herst *, Michael V. Berridge

Malaghan Institute of Medical Research, P.O. Box 7060, Wellington, New Zealand

Received 28 October 2006; received in revised form 23 November 2006; accepted 29 November 2006
Available online 6 December 2006

Abstract

Oxygen consumption for bioenergetic purposes has long been thought to be the prerogative of mitochondria. Nevertheless, mitochondrial gene knockout (ρ^0) cells that are defective in mitochondrial respiration require oxygen for growth and consume oxygen at the cell surface via trans-plasma membrane electron transport (tPMET). This raises the possibility that cell surface oxygen consumption may support glycolytic energy metabolism by reoxidising cytosolic NADH to facilitate continued glycolysis. In this paper we determined the extent of cell surface oxygen consumption in a panel of 19 cancer cell lines. Non-mitochondrial (myxothiazol-resistant) oxygen consumption was demonstrated to consist of at least two components, cell surface oxygen consumption (inhibited by extracellular NADH) and basal oxygen consumption (insensitive to both myxothiazol and NADH). The extent of cell surface oxygen consumption varied considerably between parental cell lines from 1% to 80% of total oxygen consumption rates. In addition, cell surface oxygen consumption was found to be associated with low levels of superoxide production and to contribute significantly (up to 25%) to extracellular acidification in HL60ρ^0 cells. In summary, cell surface oxygen consumption contributes significantly to total cellular oxygen consumption, not only in ρ^0 cells but also in mitochondrially competent tumour cell lines with glycolytic metabolism.

Keywords: Cell surface oxygen consumption; Aerobic glycolysis; ρ^0 cells

1. Introduction

Many aggressive and highly invasive cancers are characterized by increased reliance on glycolysis for energy production even in the presence of oxygen and this is often referred to as aerobic glycolysis or the Warburg effect [1–8]. From a bioenergetic perspective glycolysis is relatively inefficient. Nevertheless, it appears to confer a proliferative advantage on many cells, particularly those in hypoxic micro-environments often associated with early tumour development [9], compared with cells that obtain their energy through oxidative phosphorylation. High glycolytic rates in rapidly proliferating cells lead to a build up of reducing equivalents produced during glycolysis and mitochondrial TCA cycle activity. In addition to increased lactic acid production [4,10–13], highly glycolytic cells also use trans-plasma membrane electron transport (tPMET) to alleviate intracellular reductive stress [14–19]. The extent to which tPMET is employed to support aerobic glycolysis is difficult to assess in cells that use mitochondrial electron transport for at least part of their energy requirements. This issue has been addressed by employing the mitochondrial gene-knockout ρ^0 model of extreme aerobic glycolysis [14,15,18,19].

We have shown previously that human leukemia HL60 ρ^0 cells consume oxygen at the cell surface via tPMET [14]. The cell-impermeable water-soluble tetrazolium dye, WST-1, is also reduced by this tPMET system, but only in the presence of its obligate intermediate electron acceptor, 1-methoxy-5-methyl phenazinium methylsulphate (PMS) (Fig. 1). This excludes a

Abbreviations: DPI, diphenyleneiodonium; FCCP, carbonyl cyanide para-trifluoromethoxyphenylhydrazone; NOX, family of inducible NADPH-oxidases of phagocytes; NQO1, NADH:ubiquinone oxidoreductase; PMA, phorbol myristate acetate; PMS, 1-methoxy-5-methyl phenazinium methylsulphate; SOD, superoxide dismutase; tPMET, trans-plasma membrane electron transport; WST-1, 2-(4-iodophenyl)-3-(4-nitrophenyl) -5- (2,4-disulfophenyl) -2H- tetrazolium monosodium salt

* Corresponding author. Tel.: +64 4 4996914x837; fax: +64 4 4996915.
E-mail address: pherst@malaghan.org.nz (P.M. Herst).

0005-2728/$ - see front matter © 2007 Elsevier B.V. All rights reserved.
doi:10.1016/j.bbabio.2006.11.018

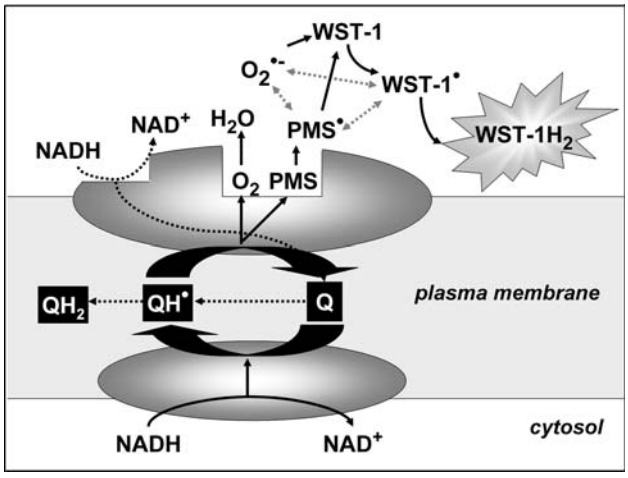

Fig. 1. Diagram of cell surface oxygen consumption and WST-1/PMS reduction. Electrons travel from intracellular NADH to extracellular oxygen or PMS via an NADH:oxidoreductase at the inner surface of the plasma membrane, the ubiquinone cycle (ubiquinone: Q and semiubiquinone: QH$^{\bullet}$) and a cell surface NADH:oxidoreductase. PMS radicals (PMS$^{\bullet}$) reduce WST-1 to a WST-1 radical (WST-1$^{\bullet}$) and then to WST-1H_2 either by PMS radicals or superoxide ($O_2^{\bullet-}$). Inhibition of cell surface oxygen consumption by NADH is postulated to be caused by reverse electron transport of electrons from extracellular NADH through the surface NADH: oxidoreductase to reduce ubiquinone to ubiquinol (QH_2).

role for the NADPH oxidase of professional phagocytes (NOX2) which, when activated by phorbol myristate acetate (PMA), reduces WST-1 directly [20]. tPMET transports electrons from intracellular NADH via an NADH: oxidoreductase at the inner surface of the plasma membrane to plasma membrane ubiquinone which then reduces extracellular oxidants via a cell surface NADH:oxidoreductase [14,21,22].

Here, we assess the extent of aerobic glycolysis in a panel of 19 human and mouse cancer cell lines by measuring their cell surface oxygen consumption rates. Non-mitochondrial oxygen consumption in ρ^0 cells has been described by various authors [15,23–27], however, the extent of this varied from very low to undetectable [23–25] to around 10–30% of parental oxygen consumption rates [15,26,28]. Significant cyanide-resistant oxygen consumption in mitochondrially competent cell lines has been reported for human lymphoblastic leukemia Molt-4 cells (60% of total oxygen consumption) [26] and CD34$^+$ hemopoietic stem cells (HSC) (40% of total oxygen consumption) [27]. Non-mitochondrial oxygen consumption in the latter was suggested to be due to superoxide production by NOX2 and NOX4 in the plasma membrane. We therefore investigated the extent to which superoxide contributes to cell surface oxygen consumption in HL60ρ^0 cells.

Increased glycolytic rates have also been associated with increased lactic acid production and extracellular acidification [4,5,13,29], although it has been claimed that lactic acid production by itself is not sufficient to explain the level of acidification in glycolytic cancer cells [4,10,12]. In order to maintain electroneutrality, increased electron transport across the plasma membrane is also associated with proton extrusion. We therefore investigated the contribution of cell surface oxygen consumption to extracellular acidification in HL60ρ^0 cells.

2. Materials and methods

2.1. Cell lines and cell culture techniques

All mammalian cell lines were grown in RPMI-1640 medium supplemented with 5% (v/v) fetal bovine serum, GlutaMAX-1 (2 mM), penicillin (100 U/mL), streptomycin sulfate (100 μg/mL), uridine (50 μg/μL) and pyruvate (1 mM) to densities of $0.5–1.0\times10^6$ cells/mL (exponential growth stage), at 37 °C in a humidified incubator maintained at 5% CO_2. The cell lines used were kind gifts from the following people: the human myeloblastic leukemia cell line, HL60, from Dr. Graeme Findley (University of Auckland, NZ); the human osteosarcoma cell lines, 143B and 143Bρ^0, from Dr. Michael P. Murphy (University of Otago, Dunedin, New Zealand); the human cervical carcinoma cell lines, HeLa, from Dr. Anthony Braithwaite (University of Otago, Dunedin, NZ); the non-adherent human cervical carcinoma cell lines, HeLaS3 and HeLaS3ρ^0, from Dr. Alfons Lawen (Monash University, Melbourne, Australia); the murine mastocytoma cell line, P815, from Dr. John. Marbrook (University of Auckland, NZ); the human monocyte-like histiocytic lymphoma cell line, U937, from American Type Culture Collection (Rockville, MD, USA); the murine myelomonocytic leukemia cell line, WEHI213, the mature murine B cell lymphoma, A20, the murine T cell lymphomas, EL4 and BW1100, the transformed murine monocyte/macrophage cell line, J774, and the transformed murine dendritic cell line, D2SC/1, from Dr. Franca Ronchese (Malaghan Institute, Wellington, NZ); the murine T cell lymphoma, BW1100, and the human acute lymphoblastic leukaemia, Jurkat, from Dr. Thomas Backström (Malaghan Institute, Wellington, NZ); the transformed human macrophage cell line, RAW264.7, from Dr. Jacquie Harper (Malaghan Institute, Wellington, NZ). HL60A (adherent) is a stable adherent cell line derived from HL60 after 48 h incubation under alkaline conditions (pH 7.8–8.2), by clonal dilutions in microplate wells. HL60ρ^0 and HeLaρ^0 were derived from their parental strains by long-term culture (6–12 weeks) with 50 ng/mL filter-sterilized ethidium bromide (EtBr) according to the protocol of King and Attardi [24] by A.S. Tan. The ρ^0 status of all ρ^0 cell lines was verified by PCR to confirm the absence of mtDNA) and by FCCP-insensitive WST-1/PMS reduction (A.S. Tan, unpublished results).

2.2. Materials

WST-1 (2-(4-iodophenyl)-3-(4-nitrophenyl)-5-(2,4-disulfophenyl)-2H-tetrazolium mono sodium salt) and PMS (1-methoxy-5methyl phenazinium methylsulphate) were purchased from Dojindo Laboratories (Kumamoto, Japan). Unless otherwise stated all other reagents were from Sigma Chemical Company (St. Louis, MO, USA).

2.3. tPMET activity as measured by WST-1/PMS reduction

For inhibitor studies, WST-1/PMS reduction rates were measured in a microplate format as described previously [17]. Briefly, exponentially growing cells were centrifuged at 130×*g* for 5 min, washed and resuspended in Hanks Balanced Salt Solution (HBSS) buffer. For each assay, 50 μL of a 2×10^6 cells/mL cell suspension was pipetted into microplate wells containing 50 μL of the inhibitor/buffer solution (10 μL of the 10× stock solution added to 40 μL of HBSS buffer), resulting in a final concentration of 1×10^6 cells/mL. Dye reduction was initiated by adding 10 μL of a 10× stock solution of WST-1/PMS in milliQ water (final concentrations of 500 μM WST-1 and 20 μM PMS). WST-1 reduction was measured in real time at 450 nM over 30–60 min in a BMG FLUOstar OPTIMA plate reader.

2.4. Superoxide production

The extent of superoxide production was measured as WST-1 reduction in the same manner as described above but in the absence of PMS [20].

2.5. Hydrogen peroxide production

The amount of hydrogen peroxide produced by cells was measured using the Amplex Red glucose/glucose oxidase kit (Molecular Probes). The assay is based on the oxidation of the Amplex Red reagent by hydrogen peroxide to form the fluorescent resorufin in the presence of horseradish peroxidase. For each experiment a

separate hydrogen peroxide standard curve (2–60 μM) was included, using the H_2O_2 standard in the kit (0.88 M hydrogen peroxide, according to the manufacturer's instructions). Reaction mixture (50 μL of a suspension containing 50 μL of 10 mM Amplex Red reagent, 100 μL of 10 U/mL horseradish peroxidase and 4.85 mL reaction buffer) was added to 50 μL of either hydrogen peroxide standards or cell supernatant. After incubation at room temperature for 10 min, resorufin appearance was measured at 560 nm in a FLUOstar Optima plate reader.

2.6. Oxygen consumption

Exponentially growing mammalian cultures were centrifuged at 130×*g* at room temperature for 5 min (Megafuge 2R Heraeus) and resuspended in fresh complete RPMI medium to a density of 2.5×10^7 cells/mL. Each experiment measured oxygen consumption by 600 μl of resuspended cells in a 1 mL chamber, surrounded by a water-filled chamber maintained at 37 °C. Oxygen consumption was measured with a Clark-type dissolved oxygen electrode, coupled to a Powerlab processor and a Macintosh computer using Powerlab software. The oxygen concentration in fully oxygenated medium and cell cultures was taken to be 200 nmol/mL (200 μM). Oxygen consumption rates were calculated in pmoles per million cells per second. For example the oxygen consumption rate for a slope of − 0.06 and 2×10^7 cells/mL was calculated as follows:

$$\frac{0.06\times 200(\text{nmol/mL})}{60(s)\times 20(10^6\ \text{cells})} = 0.01\ \text{nmol s}^{-1}10^6\ \text{cells}^{-1}\ \text{or}\ 10\ \text{pmol s}^{-1}10^6\ \text{cells}^{-1}$$

The effects of inhibitors on oxygen consumption were determined by spiking stirred cells with the specified concentration of inhibitor after a stable oxygen consumption had been achieved. Results, expressed as a percentage of control, were obtained by dividing slopes in the presence of inhibitor by control slopes within the same trace. All values were corrected for background readings obtained from fresh medium without cells (background drift).

3. Results

3.1. Cell surface oxygen consumption in glycolytic cancer cell lines

HL60ρ^0 cells have previously been shown to consume oxygen at the cell surface. In contrast, parental HL60 cells did not exhibit significant levels of cell surface O_2 consumption, raising the question of physiological relevance [14]. Here, we investigated whether cell surface oxygen consumption occurs in cells with intact mitochondrial electron transport. We therefore measured oxygen consumption in the absence and presence of myxothiazol (inhibitor of mitochondrial oxygen consumption), NADH, (inhibitor of cell surface oxygen consumption), and both myxothiazol and NADH, using a panel of 19 human and murine cancer cell lines available to us (Table 1). Interestingly, non-mitochondrial oxygen consumption was shown to consist of two distinct components, by sensitivity to extracellular NADH, previously shown to extensively inhibit oxygen consumption by HL60ρ^0 cells [14]. When comparing non-mitochondrial oxygen consumption rates in the presence and absence of NADH in different cancer cell lines, we noted a small NADH-insensitive component (between 3 and 11% of total oxygen consumption rates) in the cell lines examined. We suggest that the NADH-insensitive component of non-mitochondrial oxygen consumption is in fact a basal form of oxygen consumption, not associated with tPMET or the support of energy production.

The percentage cell surface oxygen consumption varied between 1% and 90% of total oxygen consumption among the different cell lines (Table 1). As expected, ρ^0 cell lines (HL60ρ^0, HeLaρ^0, HeLaS3ρ^0 and 143Bρ^0) showed no significant mitochondrial oxygen consumption, whereas HL60, U937, HeLa and 143B used mitochondrial oxygen consumption exclusively. In all cases, ρ^0 cells exhibited significantly lower total oxygen consumption rates than their parental counterparts (41% for HL60ρ^0, 46% for HeLaρ^0, 67% for HeLaS3ρ^0: and 34% for 143Bρ^0). Cell surface oxygen consumption in the dendritic cell line, D2SC/1 and the monocyte/macrophage cell line, J774, comprised a high percentage of total oxygen consumption rates (71% and 80% respectively), whilst other

Table 1
Comparison of WST-1/PMS reduction rates and O_2 consumption rates

Cell line	WST-1/PMS reduction	Total O_2 consumption	Mitochondrial O_2 consumption	Cell surface O_2 consumption	Basal O_2 consumption
HL60	15.25±1.26	11.46±0.40	10.59±0.40 (96%)	0.14±0.02 (1%)	0.43±0.02 (3%)
HeLa	50.85±1.61	26.86±0.85	25.25±0.84 (95%)	0.42±0.05 (1%)	1.19±0.04 (4%)
143B	29.11±2.56	16.32±0.53	15.19±0.53 (93%)	0.33±0.06 (2%)	0.81±0.02 (5%)
U937	17.48±0.99	11.00±0.83	9.90±0.53 (90%)	0.32±0.12 (3%)	0.79±0.07 (7%)
Jurkat	14.79±0.81	11.89±0.50	8.90±0.50 (75%)	2.50±0.50 (21%)	0.49±0.03 (4%)
WEHI 213	11.34±0.60	9.44±0.48	6.61±0.48 (70%)	2.35±0.15 (25%)	0.48±0.02 (5%)
RAW264.7	21.03±1.37	8.89±0.23	5.76±0.10 (66%)	2.68±0.21 (30%)	0.37±0.01 (4%)
A20	15.29±0.47	9.67±0.50	6.29±0.50 (65%)	2.91±0.17 (30%)	0.47±0.02 (5%)
EL4	11.49±0.84	7.69±0.40	4.36±0.40 (57%)	2.87±0.16 (37%)	0.46±0.02 (6%)
HeLaS3	19.51±0.90	8.42±0.32	4.54±0.32 (54%)	3.27±0.13 (39%)	0.61±0.02 (7%)
P815	13.63±0.89	5.15±0.37	2.33±0.20 (35%)	2.86±0.38 (55%)	0.53±0.04 (10%)
HL60adh	28.43±1.55	7.57±0.25	2.58±0.25 (34%)	4.44±0.16 (58%)	0.55±0.02 (7%)
BW1100	40.83±1.80	8.11±0.35	1.95±0.35 (24%)	5.43±0.26 (67%)	0.73±0.03 (9%)
D2SC/1	67.75±1.85	12.56±0.83	2.55±0.62 (20%)	8.91±0.65 (71%)	1.10±0.08 (9%)
J774	34.10±1.24	6.18±0.33	0.62±0.33 (10%)	4.95±0.30 (80%)	0.61±0.03 (10%)
HeLaρ^0	89.72±3.91	12.50±0.50	0.01±0.50 (2%)	10.70±1.25 (87%)	1.35±0.04 (11%)
143Bρ^0	41.10±1.24	5.62±0.40	0.01±0.20 (1%)	4.91±0.40 (88%)	0.72±0.04 (11%)
HL60ρ^0	30.31±1.82	4.74±0.16	0.01±0.16 (1%)	4.29±0.16 (90%)	0.44±0.03 (9%)
HeLaS3ρ^0	38.34±1.39	5.64±0.21	0.03±0.21 (1%)	4.83±0.21 (90%)	0.68±0.02 (9%)

Figures in brackets indicate percent of total O_2 consumption. WST-1/PMS reduction values are in milliA450 min^{-1} 10^5 $cells^{-1}$ and O_2 consumption rates are in pmoles O_2 s^{-1} 10^6 $cells^{-1}$. Results represents averages±SEM of three to six separate experiments.

cell lines used both mitochondrial and cell surface oxygen consumption. If the assumption is made that the purpose of cell surface oxygen consumption is to support glycolytic energy production, then it follows that 90% of the bioenergetic oxygen consumption in J774 cells and all of the bioenergetic oxygen consumption in ρ^0 cells is cell surface associated. These results challenge the current respiratory paradigm that all bioenergetic oxygen consumption in mammalian cells is mitochondrial.

There was no clear relationship between total cellular oxygen consumption and WST-1/PMS reduction (Table 1). Of the mitochondrially competent cells, the murine dendritic cell line, D2SC/1 exhibited the highest WST-1/PMS reduction but the third highest rates of total oxygen consumption. In contrast, HeLa cells had high rates of both WST-1/PMS reduction and total oxygen consumption. Because cell surface oxygen consumption uses the same tPMET system as WST-1/PMS reduction [14], we compared the rates of WST-1/PMS reduction and cell surface oxygen consumption (Fig. 2A). When all cell lines were included in the analysis, the correlation was poor ($R^2=0.5898$) but, interestingly, improved significantly ($R^2=0.98$) when cell lines that exclusively employ a mitochondrial energy metabolism (open circles in Fig. 2A) were excluded from analysis. This is an empirical observation: the reasons why some cancer cell types that are obviously capable of tPMET (as evidenced by their ability to reduce WST-1 in the presence of PMS) do not use that same system for cell surface oxygen consumption is not readily explained. It may relate to the artificial nature of the dye reduction system or to the consequences of switching from a purely mitochondrial energy metabolism to a combined mitochondrial/

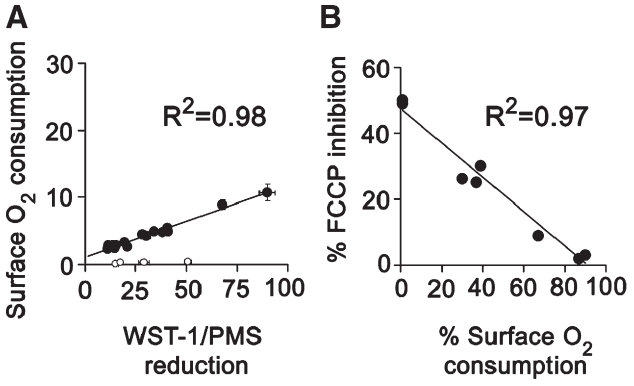

Fig. 2. (A) Relationship between WST-1/PMS reduction and cell surface oxygen consumption in different cell lines. Cell surface oxygen consumption was determined as the NADH-sensitive component of total oxygen consumption. The R^2 value in graph (A) empirically excludes those cell lines with no significant cell surface oxygen consumption (HL60, HeLa, 143B, U937). Oxygen consumption rates are in pmoles O_2 $s^{-1}10^6$ $cells^{-1}$, WST-1/PMS reduction values are in milliA450 min^{-1} 10^5 $cells^{-1}$. Results represent averages±SEM of three to six separate experiments. (B). Relationship between FCCP-inhibited WST-1/PMS reduction and cell surface oxygen consumption. The effect of FCCP (2 μM) on WST-1/PMS reduction was determined and compared with cell surface oxygen consumption. Percentage surface oxygen consumption refers to the percentage of total oxygen consumption and percentage FCCP inhibition refers to inhibition of WST-1/PMS reduction in the presence of FCCP, compared with that in the absence of FCCP. Results are the average of at least three different experiments. The following cell lines were tested; HeLa (50%), HL60 (49%), A20 (26%), EL4 (25%), HeLaS3 (30%), BW1100 (9%), HL60ρ^0 (3%), HeLaρ^0 (2%), HeLaS3ρ^0 (3%).

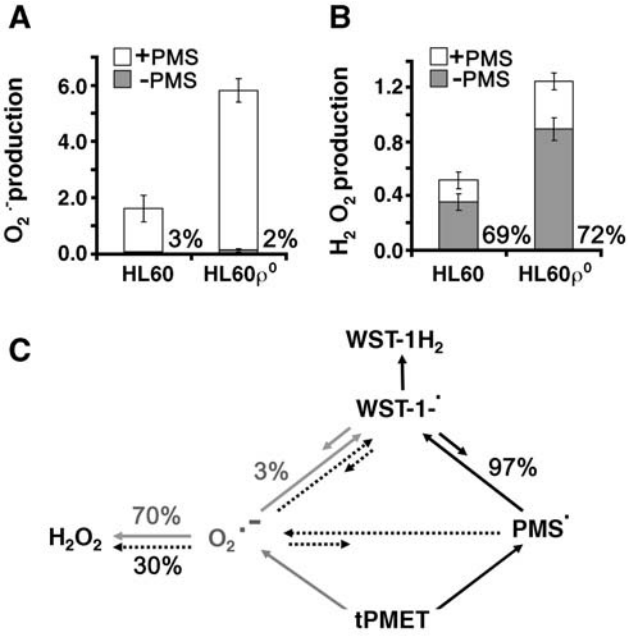

Fig. 3. Superoxide ($O_2^{\bullet -}$) production (A) and hydrogen peroxide (H_2O_2) production (B) by HL60 and HL60ρ^0 cells in the presence and absence of PMS. Superoxide production was measured as WST-1 reduction at 450 nm (milliA450 min^{-1} 10^5 $cells^{-1}$) in the presence or absence of PMS (20 μM) and H_2O_2 reduction measured as resorufin production at 560 nm (milliA560 min^{-1} 10^5 $cells^{-1}$) in the presence and absence of PMS (20 μM). Results are averages±SEM of three separate experiments and are presented as percent superoxide or hydrogen peroxide production in the absence of PMS compared to that in the presence of PMS (C). Diagram of generation of $PMS^{\bullet}$, $O_2^{\bullet -}$, H_2O_2 and WST-$1H_2$ by electrons from tPMET. Oxygen and PMS compete for electrons from tPMET. Superoxide contributed ~3% to WST-1/PMS reduction (A) and PMS radicals ($PMS^{\bullet}$) contributed ~97%. H_2O_2 is produced by dismutation of superoxide with ~70% coming directly via tPMET and ~30% originating from PMS radicals (B). This suggests that PMS-generated superoxide contributed ~1% to WST-1/PMS reduction (30% of 3%), and tPMET-generated superoxide by itself was responsible for ~2% of WST-1/PMS reduction.

glycolytic metabolism (supported by tPMET), resulting in activation in some but not all cancer cell types.

Previous work by our group has shown a strong inhibitory effect of the respiratory uncoupler, FCCP, on WST-1/PMS reduction by HL60 cells, whilst dye reduction by HL60ρ^0 cells remains unaffected [14]. Inhibition of dye reduction by FCCP in parental HL60 cells is consistent with increased mitochondrial electron transport, causing lowering of intracellular NADH levels, as shown by others. We found a strong correlation ($R^2=0.9688$) between the percentage inhibition of WST-1/PMS reduction by FCCP and the percentage of cell surface oxygen consumption (Fig. 2B). These results indicate that inhibition of WST-1/PMS reduction by FCCP may be a good measure of the extent of glycolytic metabolism.

3.2. Contribution of superoxide to cell surface oxygen consumption

Because non-mitochondrial oxygen consumption in human hemopoietic stem cells was reported to be due to superoxide production by NOX 2 and NOX 4 [27], we next examined

whether cell surface oxygen consumption might include a superoxide component. We used HL60 and HL60ρ^0 cells to model the two extremes of oxygen consumption as HL60 cells consume oxygen largely in their mitochondria and HL60ρ^0 cells use oxygen at the cell surface. Oxygen consumption, using a Clark dissolved oxygen electrode, does not distinguish between the possible end products, water and superoxide/hydrogen peroxide. One way to examine the role of superoxide in dye reduction is to utilize the ability of superoxide to reduce WST-1 directly at the cell surface [20]. We measured WST-1 reduction rates in HL60 and HL60ρ^0 cells in the presence and absence of PMS (Fig. 3A). Low levels of superoxide were detected in the absence of PMS (2–3% of the dye reduction measured in the presence of PMS). However, the contribution of superoxide to WST-1 reduction in the presence of PMS is complicated because electrons from tPMET will produce PMS radicals with both superoxide and PMS radicals existing in equilibrium, and being able to reduce WST-1 (Fig. 3C). In addition, dismutation of superoxide, accelerated by the cell-impermeable superoxide scavenger, superoxide dismutase (SOD), leads to the formation of hydrogen peroxide, resulting in lower superoxide measurements than actually produced. We therefore used Amplex Red to determine the extent of hydrogen peroxide formation in the absence and presence of PMS (Fig. 3B). HL60ρ^0 cells were found to produce 3 times as much superoxide (as measured by WST-1 reduction) and 2.5 times as much hydrogen peroxide (as measured by resorufin production) as HL60 cells. Interestingly, the addition of PMS increased resorufin production by 30% (Fig. 3B) and WST-1 reduction 30- to 50-fold (Fig. 3A,C). SOD extensively inhibited WST-1 reduction and WST-1/PMS reduction by about 70% (Table 2), indicating superoxide involvement in both reductive processes. Because WST-1/PMS reduction increases several fold in the absence of oxygen [14], involvement of superoxide in this pathway is clearly indirect. Mitochondrial oxygen consumption, as expected, was unaffected by SOD, while cell surface oxygen consumption by HL60ρ^0 cells was inhibited by 27%, possibly partially masked by superoxide dismutation and oxygen generation via SOD and catalase. Interestingly, 10 μM diphenylene iodonium (DPI), a potent NOX2 inhibitor at this concentration [30], did not affect superoxide production in either cell type. WST-1/PMS reduction and cell surface oxygen consumption were inhibited to the same extent by DPI in HL60ρ^0 cells (37% and 42% respectively), whereas mitochondrial oxygen consumption remained unaffected.

Table 2
Percentage inhibition of dye reduction and oxygen consumption

% Inhibition	25 μM SOD		10 μM DPI		2 mM Zn^{2+}	
	HL60	HL60ρ^0	HL60	HL60ρ^0	HL60	HL60ρ^0
O_2 consumption	2±3	27±8	6±3	37±4	2±4	27±9
WST-1/PMS	73±2	71±2	39±4	42±5	52±6	48±3
WST-1	97±6	96±5	5±3	3±4	ND	ND

O_2 consumption was measured in pmoles O_2 s^{-1} 10^6 $cells^{-1}$, WST-1 and WST-1/PMS reduction were measured in milliA450 min^{-1} 10^5 $cells^{-1}$. Results are averages±SEM from at least three separate experiments.

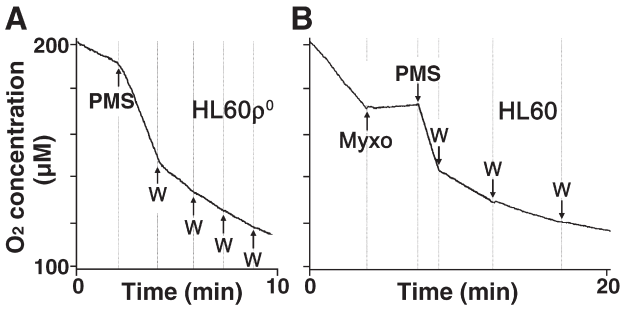

Fig. 4. Effect of PMS (20 μM), followed by WST-1 (500 μM) on oxygen consumption rates by (A) HL60ρ^0 cells and (B) on non-mitochondrial oxygen consumption by HL60 cells in the presence of myxo (myxothiazol: 1 μg/mL). Arrows indicate the points at which the various compounds were added. Results are representative of two separate experiments.

We have shown previously that PMS and oxygen compete for electrons from the same tPMET pathway and that WST-1/PMS reduction is increased by up to 4-fold under anaerobic conditions [14]. Surprisingly, PMS caused a dramatic increase in cell surface oxygen consumption in both HL60ρ^0 and HL60 cells (Fig. 4) and this has also been observed in other cell types in our laboratory (results not shown). This increased cell surface oxygen consumption was inhibited in a concentration-dependent manner by adding WST-1 (Fig. 4B). A similar inhibitory effect of WST-1 was observed in HL60 cells in the presence (Fig. 4B) and absence (results not shown) of myxothiazol. These results suggest that PMS picks up electrons from tPMET, producing PMS radicals that then efficiently reduce oxygen to superoxide, contributing to oxygen consumption. Nevertheless, as WST-1 in the presence of PMS is reduced in the absence of oxygen, PMS radicals must also efficiently reduce WST-1. We propose that WST-1, when added to this mixture, directly competes with oxygen for electrons from the PMS radicals, counteracting the PMS-induced increase in oxygen consumption at the cell surface of both HL60ρ^0 and HL60 cells (Fig. 3C).

3.3. tPMET activity contributes to acidification of the medium

We next investigated the contribution of tPMET to extracellular acidification. In order to address this issue, it is important to distinguish between proton production by LDH and by tPMET. Purely glycolytic ρ^0 cells would be expected to maximally use LDH to reoxidise NADH and consequently to produce protons stoichiometrically. If cell surface oxygen consumption contributes to medium acidification, then inhibiting this process should decrease acidification rates. Changes in acidification rates were recorded with a pH micro-electrode coupled to a Clark oxygen electrode. As expected, HL60ρ^0 cells acidified the medium much more rapidly than HL60 cells (Fig. 5A and B). Addition of NADH to HL60ρ^0 cells eliminated cell surface oxygen consumption, concomitant with a decrease in acidification rate from 0.16 to 0.12 pH units min^{-1} 10^7 $cells^{-1}$ or by 25% (Fig. 5C), and from 0.20 to 0.165 pH units min^{-1} 10^7 $cells^{-1}$, or by 18% (Fig. 5D). In contrast, the rate of acidification by HL60 cells increased after

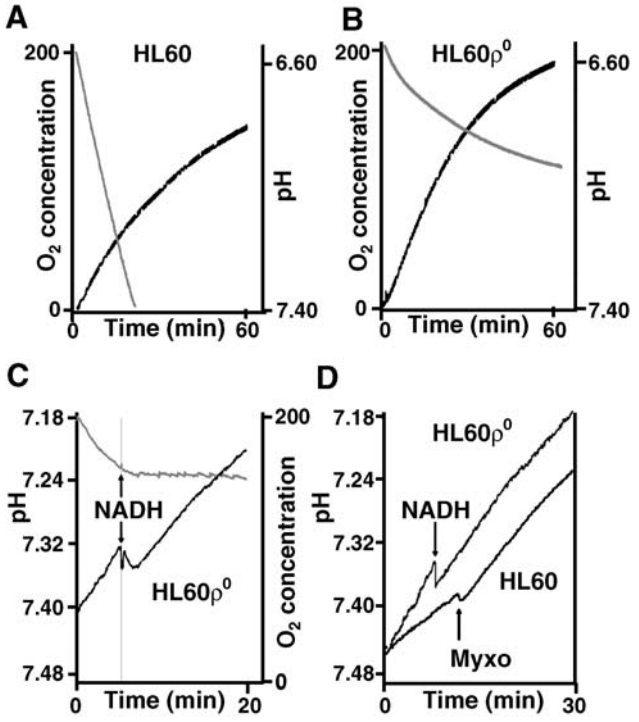

Fig. 5. Comparison of the effects of myxothiazol and NADH on oxygen consumption and acid formation by HL60 cells and HL60ρ^0 cells. HL60 cells (A) and HL60ρ^0 cells (B) were simultaneously monitored for oxygen consumption (grey traces) and pH (black traces) in a modified Clark type oxygen electrode. (C) Effect of NADH (1 mM) on oxygen consumption (grey trace) and pH changes (black trace) in HL60ρ^0 cells. (D) Effects of NADH (1 mM) and myxo (myxothiazol 1 μg/mL) on pH changes in HL60 and HL60ρ^0 cells. Results are representative of three separate experiments.

the addition of myxothiazol (from 0.075 to 0.15 pH units min^{-1} 10^7 cells^{-1}). These results demonstrate that tPMET is associated with proton extrusion and extracellular acidification, although the mechanism is unclear. Bivalent cations, such as Zn^{2+}, have been shown to extensively inhibit voltage-gated proton channels, such as those associated with NOX2 activity in phagocytes [31,32]. In support of a role for voltage-gated proton channels in tPMET, cell surface oxygen consumption in HL60ρ^0 cells and WST-1/PMS activity in both HL60 and HL60ρ^0 cells were found to be sensitive to Zn^{2+}, whereas mitochondrial oxygen consumption in HL60 cells remained unaffected (Table 2).

4. Discussion

Recent studies have shown a trend towards increased aggressiveness in cancers that are more glycolytic compared with their less glycolytic counterparts [1,3,4,8,33]. However, the extent of aerobic glycolysis in normal tissues and in tumours is controversial. Different methods have been used to distinguish between glycolysis and mitochondrial energy metabolism, making it difficult to compare results between research groups. Guppy and coworkers suggest that mitochondrial energy metabolism should be determined by oxygen consumption and glycolysis by lactic acid production [34–37]. However, as is apparent from the results presented in this paper, this would only apply to mitochondrial oxygen consumption rates and not to total oxygen consumption rates. Here, we show that non-mitochondrial (myxothiazol-resistant) oxygen consumption consists of cell surface oxygen consumption (inhibited by NADH) and basal oxygen consumption (unaffected by myxothiazol or NADH). We hypothesise that cell surface oxygen consumption rates indicate the extent of aerobic glycolysis and that these rates vary extensively between cell types (from 1% to 80% of total oxygen consumption rates in mitochondrially competent cell lines). This may, at least in part, explain the wide range of non-mitochondrial oxygen consumption rates reported in the literature, from very low or undetectable levels [23–25], to 40% of total oxygen consumption rates [15,26–28].

We further show that the extent of cell surface oxygen consumption is strongly correlated with FCCP-inhibitable WST-1/PMS reduction. This may represent a simple and reliable assay for measuring the extent of aerobic glycolysis, additional to LDH activity. Glycolytic cancers are resistant to drugs that target mitochondrially competent cells, and a simple assay that determines the extent of glycolytic metabolism in cancer cells may influence treatment options in a clinical setting.

Oxygen consumption at the cell surface raises questions about the molecular nature of this oxygen consuming system. A recent paper by Piccolo et al. described the presence of two NOX isoforms, NOX2 and NOX4, on CD34$^+$ human hemopoietic stem cells. These NADPH oxidases were constitutively expressed and could not be activated in the usual manner by PMA [27]. Cyanide-resistant oxygen consumption of up to 40% of total oxygen consumption was attributed to superoxide production by these NOX isoforms. Oxygen consumption levels in the presence of KCN were reported to be 0.83 pmoles O_2 s^{-1} 10^6 cells^{-1}. These rates are extremely low but compare well with the basal oxygen consumption rates presented in Table 1, ranging from 0.37 to 1.35 pmoles O_2 s^{-1} 10^6 cells^{-1}. This raises the intriguing possibility of NOX isoforms being present on the cell membrane of many cell lines and actively producing low levels of superoxide possibly for cell signalling purposes. This seems particularly plausible for HL60 as this is a myeloblastic leukemia cell line which, upon differentiation with dimethylsulfoxide, all–trans-retinoic acid or arsenic trioxide and stimulation with PMA, produces a significant respiratory burst, mediated by NOX2 [38] (and Herst et al., manuscript in preparation). It is conceivable that undifferentiated HL60 cells constitutively produce low levels of superoxide through NOX2. By using WST-1 reduction in the absence of PMS, we show that both HL60 and HL60ρ^0 cells produced small amounts of superoxide that was not inhibited by 10 μM DPI. In contrast, NOX2 activity is strongly inhibited by DPI at concentrations as low as 1 μM [39]. These results argue strongly against a role for NOX2 in superoxide production in HL60 and HL60ρ^0 cells. In HL60ρ^0 cells, superoxide could be produced as a result of one-electron leakage from a cell surface oxidase during cell surface oxygen consumption. However, HL60 cells do not consume oxygen at the cell surface at levels detectable by a Clark-type oxygen electrode. This suggests that electron leakage may occur at other sites on the surface oxidase

or at other sites in the tPMET system (e.g. CoQ_{10}) or that superoxide production occurs via another unrelated tPMET pathway.

The ability of highly glycolytic cells to acidify the medium has been observed in many studies [2,4,7,10–13,23,40,41]. In support of these studies, we found that glycolytic HL60ρ^0 cells acidified the medium much more rapidly than HL60 cells (Fig. 5). As expected, blocking mitochondrial oxygen consumption in HL60 cells with myxothiazol led to an approximately two-fold increase in acidification rate. Abolishing mitochondrial electron transport is expected to result in an increase in glycolytic rate with a concomitant increase in LDH activity to re-oxidise NADH. When cell surface oxygen consumption in HL60ρ^0 cells was blocked by extracellular NADH, the acidification rate decreased. This suggests that, in addition to lactic acid, cell surface oxygen consumption may account for up to 25% of the total acidification rate exhibited by HL60ρ^0 cells. These results confirm previous reports that acidification by glycolytic tumour cells is only partially due to increased lactic acid production [4,10,12]. Although there are a number of proton transport mechanisms associated with the plasma membrane, such as the N^+/H^+ antiporter, the H^+/HCO_3^- symporter and the H^+-ATPase, efficient H^+ transport also occurs via voltage-gated H^+ channels which do not use energy and are two orders of magnitude faster than other proton transporters [42]. Bivalent cations, especially Zn^{2+}, extensively inhibit voltage-gated proton channels at levels as low as 10 μM in patch-clamp experiments [42–44], and at 100–300 μM Zn^{2+} in whole cell cultures [45–47]. Zn^{2+} inhibition of WST-1/PMS reduction (IC_{50}:2 mM) and cell surface oxygen consumption (IC_{50}:4 mM) required much higher Zn^{2+} concentrations, possibly due to a difference in accessibility of Zn^{2+} binding sites. These results do not distinguish between direct inhibition by Zn^{2+} binding to the active site of the surface NADH: oxidoreductase of the tPMET system, or indirect inhibition by Zn^{2+} binding to associated voltage-gated H^+ channels. In the latter case, abolishing H^+ extrusion would inhibit tPMET by compromising electroneutrality during electron transport across the cell membrane. Although these results suggest involvement of voltage-gated H^+ channels in the acidification associated with tPMET, a role for other proton transport mechanisms cannot be excluded.

In summary, we have shown here that the extent of cell surface oxygen consumption varies extensively between different cancer cell lines and that this is directly related to the percentage FCCP-inhibited WST-1/PMS reduction. We propose that the best method of determining the extent of mitochondrial energy production is to measure myxothiazol-inhibited oxygen consumption and not total oxygen consumption as previously suggested [37]. We show that the extent of aerobic glycolysis may be related to cell surface oxygen consumption or the percentage FCCP-inhibited WST-1/PMS reduction. We also showed that HL60 and HL60ρ^0 cells produced low levels of superoxide, which contributed only marginally to cell surface oxygen consumption and that superoxide production was unlikely to be mediated by any of the NOX isoforms. Cell surface oxygen consumption was further demonstrated to contribute up to 25% to extracellular acidification in HL60ρ^0 cells, possibly via voltage-gated proton channels.

Acknowledgements

This research was supported by grants from the Cancer Society of New Zealand, the New Zealand Marsden Fund, the Department of Radiation Therapy, Wellington School of Medicine and Health Sciences, University of Otago, New Zealand.

References

[1] I.F. Robey, A.D. Lien, S.J. Welsh, B.K. Baggett, R.J. Gillies, Hypoxia-inducible factor-1alpha and the glycolytic phenotype in tumors, Neoplasia 7 (2005) 324–330.
[2] E. Bustamante, H.P. Morris, P.L. Pedersen, Energy metabolism in cancer cells: requirement for a form of hexokinase with a propensity for mitochondrial binding, J. Biol. Chem. 256 (1981) 8699–8704.
[3] H. Simonnet, N. Alazard, K. Pfeiffer, C. Gallou, C. Béroud, J. Demont, R. Bouvier, H. Schägger, C. Godinot, Low mitochondrial respiratory chain content correlates with tumor aggressiveness in renal cell carcinoma, Carcinogenesis 23 (2002) 759–768.
[4] P.A. Schornack, R.J. Gillies, Contributions of cell metabolism and H^+ diffusion to the acidic pH of tumors, Neoplasia 5 (2003) 135–145.
[5] O. Warburg, Ist die Glykolyse spezifisch für die Tumoren? Biochem. Z. 204 (1929) 482–483.
[6] E. Bustamante, P.L. Pedersen, High aerobic glycolysis of rat hepatoma cells in culture: role of mitochondrial hexokinase, Proc. Natl. Acad. Sci. U. S. A. 74 (1977) 3735–3739.
[7] R.L. Elstrom, D.E. Bauer, M. Buzzai, R. Karnauskas, M.H. Harris, D.R. Plas, H. Zhuang, R.M. Cinalli, A. Alavi, C.M. Rudin, C.B. Thompson, Akt stimulates aerobic glycolysis in cancer cells, Cancer Res. 64 (2004) 3892–3899.
[8] M. Kunkel, T.E. Reichert, P. Benz, H.A. Lehr, J.H. Jeong, S. Wieand, P. Bartenstein, W. Wagner, T.L. Whiteside, Overexpression of Glut-1 and increased glucose metabolism in tumors are associated with a poor prognosis in patients with oral squamous cell carcinoma, Cancer 97 (2003) 1015–1024.
[9] R.A. Gatenby, R.J. Gillies, Why do cancers have high aerobic glycolysis? Nat. Rev., Cancer 4 (2004) 891–899.
[10] M. Yamagata, K. Hasuda, T. Stamato, I.F. Tannock, The contribution of lactic acid to acidification of tumours: studies of variant cells lacking lactate dehydrogenase, Br. J. Cancer 77 (1998) 1726–1731.
[11] K. Brand, Aerobic glycolysis by proliferating cells: protection against oxidative stress at the expense of energy yield, J. Bioenerg. Biomembr. 29 (1997) 355–364.
[12] K. Newell, A. Franchi, J. Pouyssegur, I. Tannock, Studies with glycolysis-deficient cells suggest that production of lactic acid is not the only cause of tumor acidity, Proc. Natl. Acad. Sci. U. S. A. 90 (1993) 1127–1131.
[13] P.L. Pedersen, Tumor mitochondria and the bioenergetics of cancer cells, Prog. Exp. Tumor Res. 22 (1978) 190–274.
[14] P.M. Herst, A.S. Tan, D.-J.G. Scarlett, M.V. Berridge, Cell surface oxygen consumption by mitochondrial gene knockout cells, Biochim. Biophys. Acta 1656 (2004) 79–87.
[15] J.A. Larm, F. Vaillant, A.W. Linnane, A. Lawen, Up-regulation of the plasma membrane oxidoreductase as a prerequisite for the viability of human Namalwa rho 0 cells, J. Biol. Chem. 269 (1994) 30097–30100.
[16] J.M. Villalba, P. Navas, Plasma membrane redox system in the control of stress-induced apoptosis, Antiox. Redox Signal. 2 (2000) 213–230.
[17] M.V. Berridge, A.S. Tan, High-capacity redox control at the plasma membrane of mammalian cells: trans-membrane, cell surface, and serum NADH-oxidases, Antiox. Redox Signal. 2 (2000) 231–242.

[18] M.V. Berridge, A.S. Tan, Cell-surface NAD(P)H-oxidase: relationship to trans-plasma membrane NADH-oxidoreductase and a potential source of circulating NADH-oxidase, Antiox. Redox Signal. 2 (2000) 277–288.
[19] D.-J. Scarlett, P. Herst, A. Tan, C. Prata, M. Berridge, Mitochondrial gene-knockout (rho0) cells: a versatile model for exploring the secrets of trans-plasma membrane electron transport, Biofactors 20 (2004) 199–206.
[20] A.S. Tan, M.V. Berridge, Superoxide produced by activated neutrophils efficiently reduces the tetrazolium salt, WST-1 to produce a soluble formazan: a simple colorimetric assay for measuring respiratory burst activation and for screening anti-inflammatory agents, J. Immunol. Methods 238 (2000) 59–68.
[21] M.V. Berridge, P.M. Herst, A.S. Tan, Tetrazolium dyes as tools in cell biology: new insights into their cellular reduction, Biotechnol. Annu. Rev. 11 (2005) 127–152.
[22] D.-J.G. Scarlett, P.M. Herst, M.V. Berridge, Multiple proteins with single activities or a single protein with multiple activities: the conundrum of cell surface NADH oxidoreductases, Biochim. Biophys. Acta 1708 (2005) 108–119.
[23] R. Fukuyama, A. Nakayama, T. Nakase, H. Toba, T. Mukainaka, H. Sakaguchi, T. Saiwaki, H. Sakurai, M. Wada, S. Fushiki, A newly established neuronal rho-0 cell line highly susceptible to oxidative stress accumulates iron and other metals, J. Biol. Chem. 277 (2002) 41455–41462.
[24] M.P. King, G. Attardi, Human cells lacking mtDNA: repopulation with exogenous mitochondria by complementation, Science 246 (1989) 500–503.
[25] D. Loiseau, A. Chevrollier, O. Douay, F. Vavasseur, G. Renier, P. Reynier, Y. Malthiery, G. Stepien, Oxygen consumption and expression of the adenine nucleotide translocator in cells lacking mitochondrial DNA, Exp. Cell Res. 278 (2002) 12–18.
[26] J. Shen, N. Khan, L.D. Lewis, R. Armand, O. Grinberg, E. Demidenko, H. Swartz, Oxygen consumption rates and oxygen concentration in Molt-4 cells and their mtDNA depleted (ρ^0) mutants, Biophys. J. 84 (2003) 1291–1298.
[27] C. Piccoli, R. Ria, R. Scrima, O. Cela, A. D'Aprile, D. Boffoli, F. Falzetti, A. Tabilio, N. Capitanio, Characterisation of mitochondrial and extra-mitochondrial oxygen consumption reactions in human hematopoietic strem cells: novel evidence of the occurrence of NAD(P)H oxidase activity, J. Biol. Chem. 280 (2005) 26467–26476.
[28] J.A. Larm, E.J. Wolvetang, F. Vaillant, R.D. Martinus, A. Lawen, A.W. Linnane, Increase of plasma membrane oxidoreductase activity is not correlated with the production of extracellular superoxide radicals in human Namalwa cells, Protoplasma 184 (1995) 173–180.
[29] O. Warburg, On the origin of cancer cells, Science 123 (1956) 309–314.
[30] L.M. Henderson, J.B. Chappel, NADPH oxidase of neutrophils, Biochim. Biophys. Acta 1273 (1996) 87–107.
[31] T.E. DeCoursey, D. Morgan, V.V. Cherny, The voltage-dependence of NADPH oxidase reveals why phagocytes need proton channels, Nature 422 (2003) 531–534.
[32] L.M. Henderson, R.W. Meech, Evidence that the product of the human X-linked CGD gene, $gp91^{phox}$ is a voltage gated H^+ pathway, J. Gen. Physiol. 114 (1999) 771–785.
[33] S. Yasuda, S. Arii, A. Mori, N. Isobe, W. Yang, H. Oe, A. Fujimoto, Y. Yonenaga, H. Sakashita, M. Imamura, Hexokinase II and VEGF expression in liver tumors: correlation with hypoxia-inducible factor-1α and its significance, J. Hepatol. 40 (2004) 117–123.
[34] M. Guppy, The hypoxic core: a possible answer to the cancer paradox, Biochem. Biophys. Res. Commun. 299 (2002) 676–680.
[35] M. Guppy, S. Brunner, M. Buchanan, Metabolic depression: a response of cancer cells to hypoxia? Comp. Biochem. Physiol., Part B: Biochem. Mol. Biol. 140 (2005) 233–239.
[36] M. Guppy, P. Leedman, X. Zu, V. Russell, Contribution by different fuels and metabolic pathways to the total ATP turnover of proliferating MCF-7 breast cancer cells, Biochem. J. 364 (2002) 309–315.
[37] X.L. Zu, M. Guppy, Cancer metabolism, facts, fantasy, and fiction, Biochem. Biophys. Res. Commun. 313 (2004) 459–465.
[38] P.M. Herst, D.M. Levine, M.V. Berridge, Mitochondrial gene knockout $HL60\rho^0$ cells show preferential differentiation into monocytes/macrophages, Leuk. Res. 29 (2005) 1163–1170.
[39] A.K. Robertson, A.R. Cross, O.T. Jones, P.W. Andrew, The use of diphenylene iodonium, an inhibitor of NADPH oxidase, to investigate the antimicrobial action of human monocyte derived macrophages, J. Immunol. Methods 133 (1990) 175–179.
[40] K.A. Frauwirth, C.B. Thompson, Regulation of T lymphocyte metabolism, J. Immunol. 172 (2004) (46646614665).
[41] T. Cramer, Y. Yamanishi, B.E. Clausen, I. Förster, R. Pawlinski, N. Mackman, V.H. Haase, R. Jaenisch, M. Corr, V. Nizet, G.S. Firestein, H.P. Gerber, N. Ferrara, R.S. Johnson, HIF-1alpha is essential for myeloid cell-mediated inflammation [erratum appears in Cell. 2003 May 2;113(3):419], Cell 112 (2003) 645–657.
[42] T.E. DeCoursey, V.V. Cherny, Common themes and problems of bioenergetics and voltage-gated proton channels, Biochim. Biophys. Acta 1458 (2000) 104–119.
[43] T.E. DeCoursey, V.V. Cherny, Voltage-activated hydrogen currents, J. Membr. Biol. 141 (1994) 203–233.
[44] V.V. Cherny, T.E. DeCoursey, pH-Dependent inhibition of voltage-gated H^+ currents in rat alveolar epithelial cells by Zn^{2+} and other divalent cations, J. Gen. Physiol. 114 (1999) 819–838.
[45] L.M. Henderson, S. Thomas, G. Banting, J.B. Chappel, The arachidonate-activatable, NADPH oxidase-associated H^+ channel is contained within the multi-membrane-spanning N-terminal region of $gp91^{phox}$, Biochem. J. 701 (1997) 701–705.
[46] L.M. Henderson, Role of histidines identified by mutagenesis in the NADPH oxidase-associated H^+ channel, J. Biol. Chem. 273 (1998) 33216–33223.
[47] T.J. Mankelov, L.M. Henderson, Inhibition of the neutrophil NADPH oxidase and associated H^+ channel by diethyl pyrocarbonate (DEPC), a histidine-modifying agent: evidence for at least two sites, Biochem. J. 358 (2001) 315–324.